

Field measurement and numerical simulation of excavation damaged zone in a 2000 m-deep cavern

Yuting Zhang*, Xiuli Ding, Shuling Huang, Yang Qin, Peng Li and Yujie Li

Key Laboratory of Geotechnical Mechanics and Engineering of the Ministry of Water Resources,
Changjiang River Scientific Research Institute, Wuhan, 430010, China

(Received June 4, 2018, Revised July 19, 2018, Accepted July 30, 2018)

Abstract. This paper addresses the issue of field measurement of excavation damage zone (EDZ) and its numerical simulation method considering both excavation unloading and blasting load effects. Firstly, a 2000 m-deep rock cavern in China is focused. A detailed analysis is conducted on the field measurement data regarding the mechanical response of rock masses subjected to excavation and blasting operation. The extent of EDZ is revealed 3.6 m-4.0 m, accounting for 28.6% of the cavern span, so it is significantly larger than rock caverns at conventional overburden depth. The rock mass mechanical response subjected to excavation and blasting is time-independent. Afterwards, based on findings of the field measurement data, a numerical evaluation method for EDZ determination considering both excavation unloading and blasting load effects is presented. The basic idea and general procedures are illustrated. It features a calibration operation of damage constant, which is defined in an elasto-plastic damage constitutive model, and a regression process of blasting load using field blasting vibration monitoring data. The numerical simulation results are basically consistent with the field measurement results. Further, some issues regarding the blasting loads, applicability of proposed numerical method, and some other factors are discussed. In conclusion, the field measurement data collected from the 2000 m-deep rock cavern and the corresponding findings will broaden the understanding of tunnel behavior subjected to excavation and blasting at great depth. Meanwhile, the presented numerical simulation method for EDZ determination considering both excavation unloading and blasting load effects can be used to evaluate rock caverns with similar characteristics.

Keywords: rock cavern; field measurement; excavation damaged zone (EDZ); numerical simulation; blasting load

1. Introduction

Rock excavation is a necessary procedure for the construction of rock underground projects but it produces noticeable adverse impacts on the surrounding rocks. The produced impacts are mainly caused by blasting and subsequent unloading of the natural stress in rock masses. Due to the removal of rocks, the equilibrium state of natural stress is disturbed and changed to a secondary stress field. During the stress variation process, the stress state in rocks near excavation surfaces changes drastically and causes tensile and shear failures in surrounding rocks. As a result, the mechanical properties of the nearby rock masses are severely deteriorated. On a microscopic scale, the deterioration is manifested by the open of original tiny fissures and the presence of invisible cracks of rocks near excavation surfaces. On a macroscopic scale, it undermines the integrity of rocks near excavation surfaces and accounts for the decrease of rock mass bearing capacity, which is usually measured by the deformation and strength characteristics of rock masses. The deteriorated rocks in the vicinity of excavation surfaces are generally termed as excavation damaged zone (EDZ). A large number of

engineering practices reveal that the extent of EDZ is a key index for the evaluation of rock mass stability and an essential basis for the design of rock support (Liu *et al.* 2013, Chen *et al.* 2016, Wang *et al.* 2016, Li *et al.* 2017). Therefore, the formation mechanism of EDZ and its quantitative determination method (Bobet 2009, Lesparre *et al.* 2013) are always a focus for engineers and scholars in the scope of rock mechanics.

The borehole acoustic emission method serves as a widely adopted technique to quantify the extent of EDZ and to assess the quality of excavation (Li *et al.* 2011, Gholizadeh *et al.* 2015). This method uses the velocity of longitudinal wave transmitted in rock masses as an indicator of rock mass quality (Jin *et al.* 2017). Because it is common engineering knowledge that the velocity magnitude remains basically unchanged in undamaged rock masses with similar lithological and rock mass structure characteristics and decreases when rock masses are physically degraded. The extent of EDZ is then determined according to the range of rocks where decreased velocity is identified.

The study of EDZ has received considerable attention and fruitful achievements were made regarding the formation mechanism (Tokiwai *et al.* 2013, Jeon *et al.* 2015), testing technique (Christaras and Chatziangelou 2014), and numerical evaluation method (Yang *et al.* 2015, Han *et al.* 2016, Song *et al.* 2018) of EDZ. These researches mainly focus on the role of excavation unloading effect in the formation process of EDZ. Although there are also

*Corresponding author, Associate Professor
E-mail: magicdonkey@163.com

many excellent studies on the analysis of blasting induced impact on engineering structures (Bayraktar *et al.* 2010), buildings, slope and tunnel rocks, their main interests involve the mechanisms of blasting effect and its influences (Almusallam *et al.* 2010, Liang *et al.* 2013, Xue *et al.* 2013, Oncu *et al.* 2015, Toy and Sevim, 2017). So far, for rocks surrounding an underground cavern, little attention was drawn to the joint effects of blasting and unloading on the characteristics of EDZ. It should be noted that the drilling and blasting method, as one of the major construction methods for rock excavation, is widely used for a variety of rock projects. The blasting seismic waves triggered by explosives can not only cause the vibration of surrounding rocks during wave propagation, but also contribute to the initiation and development of fissures in rock masses and the formation of visible macroscopic cracks. Therefore, the adverse effect of blasting on the surrounding rocks is unavoidable. Although the action time of blasting load is short, it may aggravate the relaxation degree of nearby rocks, resulting in a further decrease of rock mass quality and bearing capacity, thus making the stability of surrounding rocks even more unfavorable.

Based on the above understanding, this paper focuses on a 2000m-deep rock cavern in China and employs both experimental and numerical method to investigate the development of EDZ during construction process and propose an EDZ evaluation method considering both blasting and unloading effects. The aim of this work is to provide useful information of the measured characteristics of EDZ of surrounding rocks buried at great depth, to suggest an effective procedure for numerically evaluating the various effects induced by drilling and blasting method, and finally to deliver both documentary and theoretical references for other rock excavation projects.

2. Field tests and monitoring in the 2000 m-deep rock cavern and result analysis

2.1 Project outline

The Jinping II hydropower plant is located on the Yalongjiang river in Sichuan Province, China. Its total installed capacity is 4800 MW. The project was started in January, 2007 and completed in December, 2012. 4 headrace tunnels are excavated and their average length is 16.7 km. Two single-lane auxiliary construction tunnels, which are parallel to the headrace tunnels, serves as the traffic tunnels during construction period and are 17.5 km in length. The overburden depth of the auxiliary construction tunnels ranges from 1500 m to 2000 m and the maximum is 2375 m. During the construction period of hydropower plant, the favorable condition of the deeply buried headrace tunnels and auxiliary construction tunnels attracts the attentions of scientists of various background. An underground space of 40 m long, 6 m wide, and 6 m high was excavated on the sidewall of one auxiliary construction tunnel to provide a unique site for some basic frontier studies, such as dark matter detection, neutrino experiments, and other subjects related to the area of particle physics and astrophysics. This is the very origin of Jinping Underground

Laboratory. In 2014, the Phase II of Jinping Underground Laboratory commenced in response to the increasing needs of basic physics and related disciplines as while as the aim to look into a series of rock mechanics problems encountered in the operation of long distance water conveyance tunnels with great overburden depth. In Phase II project, the sidewall of 1# auxiliary construction tunnel was further excavated to build four experiment tunnels and some connection tunnels. Within each experiment tunnels two laboratories are allocated so eight laboratories are built in total.

The underground laboratories are located in the deepest area of Jinping Mountain with a general overburden depth exceeding 2000 m. This paper focuses on the construction process of Phase II project and carries out a comprehensive analysis on the data obtained through field monitoring and tests. The vibration response of rock masses under blasting effect as well as the relaxation characteristics of surrounding rocks after excavation are both studied. The field monitoring data and test results provide solid materials for studying the evaluation method considering both blasting and unloading effects.

2.2 Engineering and geological conditions

The Phase II project of Jinping Underground Laboratory is 9.5 km and 8.0 km distant to the eastern portal and western portal of the auxiliary construction tunnel, respectively. The dark matter laboratory that has been put into operation is about 600 m distant from the Phase II project site. The Phase II project consists of four experiment tunnels and each cavern is 130 m long. There are two 65 m-long laboratories in each cavern. Fig. 1 plots the layout of #1~#4 experiment tunnels and #1~#8 laboratories. The longitudinal axis orientation is N58W°, which is parallel to the auxiliary construction tunnel. The cross-section profile of experiment tunnel is D-shaped with a dimension of 14 m×14 m. The net distance between the #1 and #3 experiment tunnels and the auxiliary construction tunnel is 60 m, and two access tunnels with a floor slope ratio of 0.5% connect them. The net distance between the #2 and #4 experiment tunnels and the auxiliary construction tunnel is 134 m, and two access tunnels with a floor slope ratio of 4.5% connect them.

The Phase II project site is located in Baishan formation marble. The surrounding rock integrity degree is classified as medium to unfavorable. The rocks are mainly slightly weathered but the areas along the fault zone and erosion zone are weakly to strongly weathered. The underground water mainly takes the form of dripping and strand flow. According to the site geological conditions revealed by auxiliary construction tunnels, the rock masses are mainly classified as the second to the third level (there are five levels in total and the best is the first level) on basis of the standard for the engineering classification of rock masses (The National Standards Compilation Group of the P.R.C., 2015). The hydraulic fracturing method was used in the auxiliary construction tunnel to measure rock mass stress and the results indicate that the maximum principal stress reaches 70 MPa, which is an extremely high natural stress magnitude. The uniaxial compressive strength for saturated

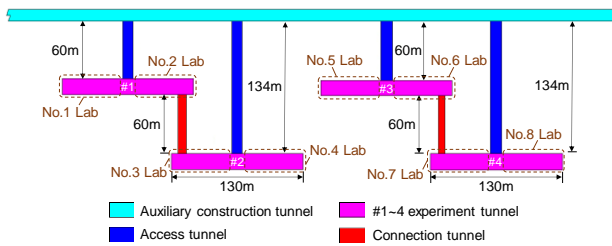


Fig. 1 Location and plan view of the Phase II of Jinping Underground Laboratory

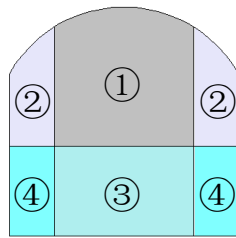


Fig. 2 Excavation step of the experiment tunnels

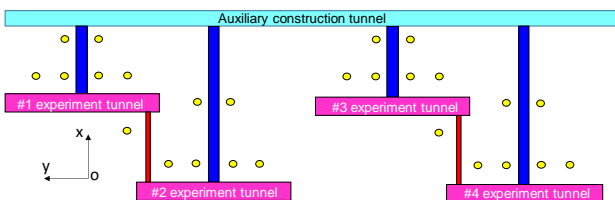


Fig. 3 Plan view of the distribution of pre-installed instrument (denoted as yellow circles) for blasting vibration monitoring

marble samples ranges from 65 MPa to 90 MPa and the tensile strength ranges from 3 MPa to 6 MPa. Therefore, the ratio of strength to stress, which is defined as the ratio of compressive stress to natural stress, is smaller than 2 for most rock masses at the project site.

2.3 Field test of rock mass vibration subjected to blasting effect

2.3.1 Plan of blasting vibration monitoring

The excavation of each experiment tunnels consists of four steps (Fig. 2). The first step is excavating the pilot tunnel. The second step is excavating the sidewalls of the pilot tunnel to enlarge the cross-section of the experiment tunnels. The third step is excavating the middle part of the floor and the fourth step is excavating the remaining part of the floor. The drilling and blasting method is adopted. The blasting scheme, including the layout of blast hole, the amount of dynamite, and the detonating network, is obtained based on the blasting quality optimization through trial blasting at the start of each excavation step.

In order to study the vibration characteristics of rock masses and the transmission characteristics of blasting seismic wave, two types of monitoring instruments are adopted. They are pre-installed instruments and surface random instruments. The pre-installed instruments are installed inside the holes on sidewalls of rock mass before blasting operation. The holes where pre-installed

instruments are placed are drilled from neighboring tunnels and their layout is plotted in Fig. 3. The surface random instruments are installed along with the blasting and excavation construction to provide more information for areas of special concern and particular significance. The vibration velocity is measured along three directions that are perpendicular to each other. The x axis shown in Fig. 3 points to the direction perpendicular to the longitudinal direction of the construction auxiliary tunnel. The y axis is consistent to the longitudinal direction and the z axis is the vertical direction.

2.3.2 Analysis of the blasting vibration monitoring results

The peak particle velocity (PPV) *versus* the distance to explosion source are plotted in Fig. 4. Surface random instruments obtain the plotted data and the distance to explosion source refers to the distance between the monitoring instruments and the site of explosion. The obtained PPV values distribute in 0.25~14.47 cm/s in x direction, 0.28~13.93 cm/s in y direction, and 0.46~7.77 cm/s in z direction. Fig. 5 plots the PPV values based on pre-installed instruments and the magnitudes distribute in 0.27~11.61 cm/s in x direction, 0.27~10.67 cm/s in y direction, and 0.02~12.66 cm/s in z direction. The distribution of PPV values, based on blasting monitoring results, shows a certain degree of dispersion. That is, the monitored PPV values are different when the distances to explosive source are identical. The possible reasons lie in the following three aspects based on analyzing the field conditions.

(1) The drilling and blasting excavation is conducted rationally as the face advances. As rock mass properties and field stress vary to a certain extent from place to place, the transmission characteristics of blasting seismic wave will be somewhat affected and thus produce different effects on rock masses, causing the dispersion of vibration magnitude.

(2) The rock mass contains various geological discontinuities, including fissures, fractures, joints, and weak interlayers, which determines the heterogeneous nature and differentiate rock mass from man-made materials. Therefore, the geological discontinuities inevitably affect the transmission characteristics of blasting seismic wave and cause the dispersion of vibration magnitudes of rock masses.

(3) The location where blasting vibration data are collected has direct impact to the recorded magnitude of rock mass vibration. As free surface amplification effect will be present when blasting seismic wave arrives at excavation surfaces, the data collected by surface random instruments will be amplified. Moreover, the amplification effect is more remarkable for instruments installed at tunnel intersections, causing even larger vibration magnitudes. On the contrary, the pre-installed monitoring instruments are installed inside the rock mass where amplification effect is absent. Therefore, the instrument installation location plays an important role in the distribution of monitored PPV. Inclusion of this factor certainly contributes to the dispersion of PPV values plotted in Figs. 4 and 5.

The monitored PPV values obtained by different kind of monitoring instruments are further compared. It is shown that the degree of dispersion of PPV values *versus* distance

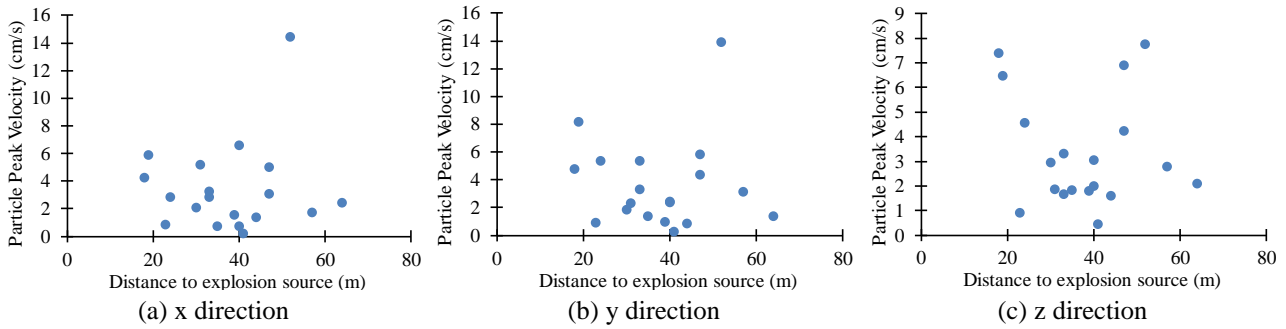


Fig. 4 Monitoring results collected by surface random instruments during 1st excavation step

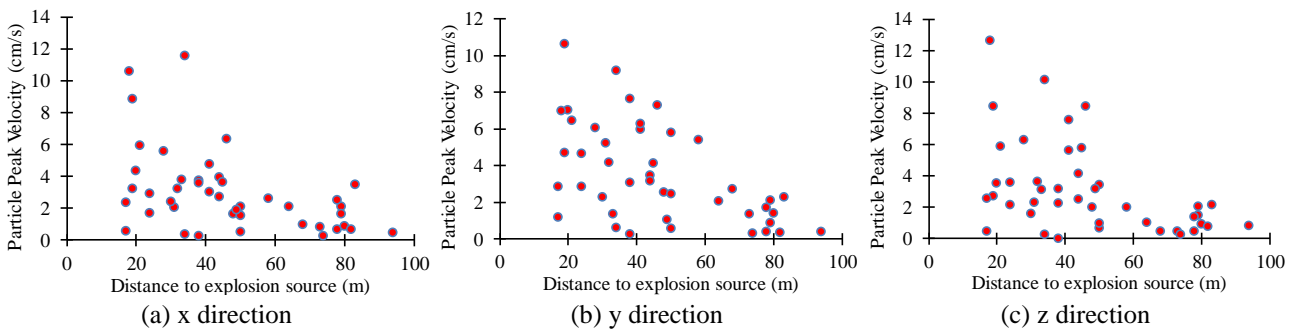


Fig. 5 Monitoring results collected by pre-installed instruments during 1st excavation step

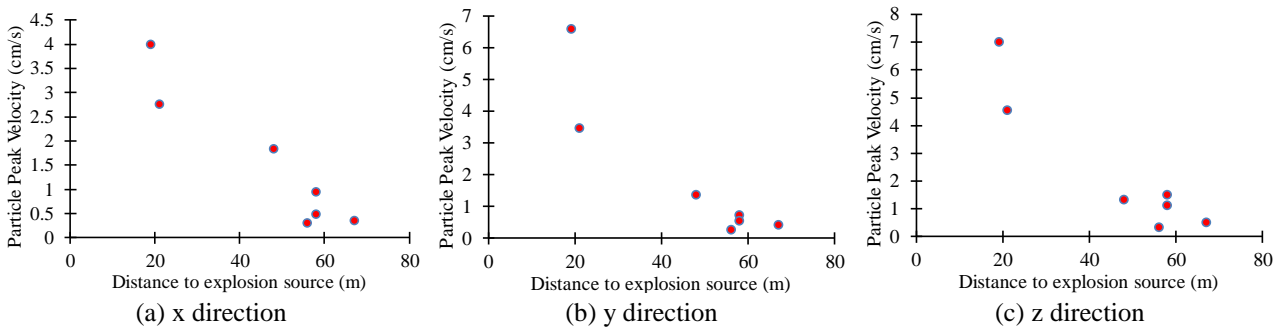


Fig. 6 Monitoring results collected by pre-installed instruments during 3rd excavation step

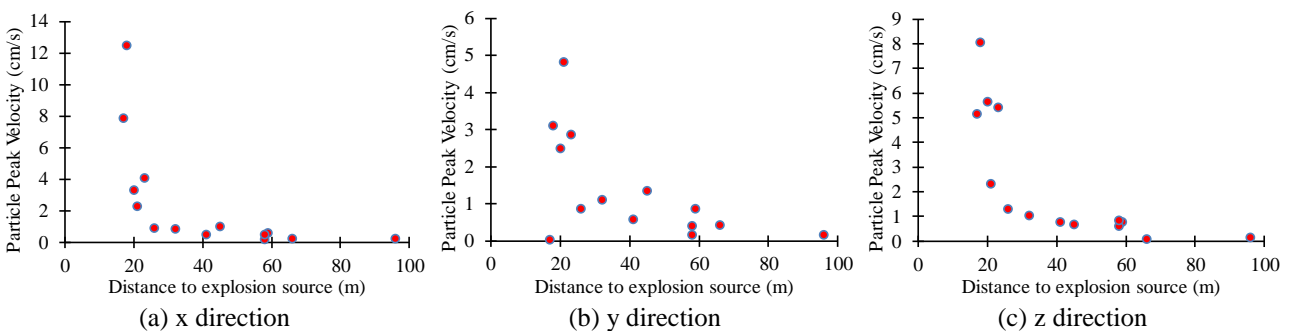


Fig. 7 Monitoring results collected by pre-installed instruments during 4th excavation step

to explosion source collected by pre-installed instruments is lower than the data collected by surface random instruments. It is probably because the surface random monitoring instruments are placed at the surface of excavation and thus receive much more construction disturbance than the pre-installed instruments do. Hence, the data collected by pre-installed instruments are viewed as

primary basis for evaluating rock mass vibration.

Fig. 6 and Fig. 7 plot the PPV values *versus* distance to explosion collected by pre-installed instruments during subsequent excavation steps. The data monitored during the third step show that the PPV distributes in 0.31~4.0 cm/s in x direction, 0.27~6.6 cm/s in y direction, and 0.34~7.02cm/s in z direction, when the distance to

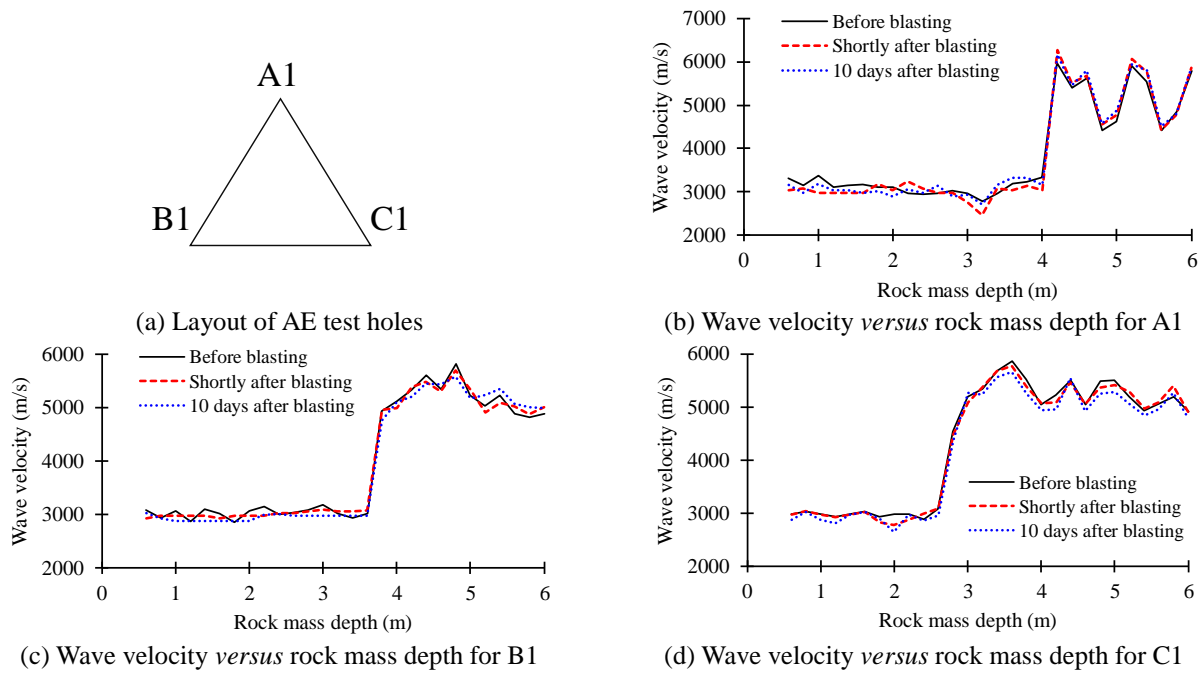


Fig. 8 Acoustic emission tests at the left sidewall of #3 Laboratory (Sta. 0+45m)

Table 1 Summary of AE test performed at the left sidewall of No. 3 Lab (Sta. 0+45m)

AE testing holes and their testing time	EDZ (m)	Wave velocity of whole length (m/s)	Average wave velocity (m/s)		
			Whole length	Within EDZ	Outside EDZ
A1	Before blasting	2780~5980	3874	3104	5261
	Shortly after blasting	2457~6270	3848	3002	5370
	10 days after blasting	2710~6160	3884	3052	5379
B1	Before blasting	2850~5820	3952	3025	5187
	Shortly after blasting	2933~5701	3935	3009	5170
	10 days after blasting	2873~5590	3911	2945	5200
C1	Before blasting	2886~5861	4361	2981	5253
	Shortly after blasting	2781~5781	4338	2957	5231
	10 days after blasting	2657~5657	4256	2905	5130

explosion source ranges from 19 m to 67 m. The data monitored during the fourth step show that the PPV distributes in 0.19~12.5 cm/s in x direction, 0.03~4.82 cm/s in y direction, and 0.09~8.07 cm/s in z direction, when the distance to explosion source ranges from 17 m to 96 m. It is observed that the rock mass vibration magnitudes in x and z directions are larger.

Although the amount of monitored data in the third and fourth steps are smaller, the obtained distribution of PPV values shows more regularity.

2.4 Acoustic emission tests on surrounding rocks during excavation process

2.4.1 Scheme of acoustic emission tests

The acoustic emission (AE) tests are carried out along

with the excavation process of experiment tunnels. The tests use the probe with one transmitter and four receivers and the test interval inside rock masses is 0.2 m. For each test there are three testing holes distributing in a triangle layout with 1m distance to each other (Fig. 8(a)) and the holes are 76 mm in diameter. The depth of each test hole is required to reach 10 m but the actual depth is about 5~6 m due to some site restrictions. The AE tests are carried out at the sidewall of experiment tunnel and the test holes are roughly 1 m above the cavern floor. The distance between the test holes and the explosion source is about 10 m. 30 AE tests are carried out in total along with the excavation process using drilling and blasting method.

2.4.2 Analysis of the AE test results

The representative AE test results are analyzed at first. Fig. 8(b)-8(d) plots the curves of longitudinal wave velocity versus rock mass depth at the location of left sidewall, Sta. 0+45 m in #3 Laboratory. Table 1 summarizes the results of AE test.

It is observed that the wave velocity is considerably low at the areas close to excavation surfaces and the magnitudes are smaller than 3000 m/s, while the value is high at the areas far from the excavation surfaces and the magnitudes are all larger than 5500 m/s. This indicates that the rock masses become less affected as the distance to excavation and fewer disturbance caused by blasting and unloading as they become more and more distant from the excavation surfaces. Therefore, based on the AE test results, the areas where high wave velocity magnitudes are measured can be deems as natural and undisturbed rock masses. The areas where low wave velocity magnitudes are measured, in comparison with the natural rock masses, are considerably affected by blasting and excavation unloading and form excavation damage zone, which is usually abbreviated as EDZ.

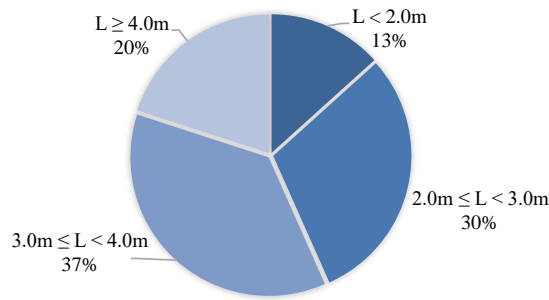


Fig. 9 Summary of monitored depths of EDZs derived from AE tests

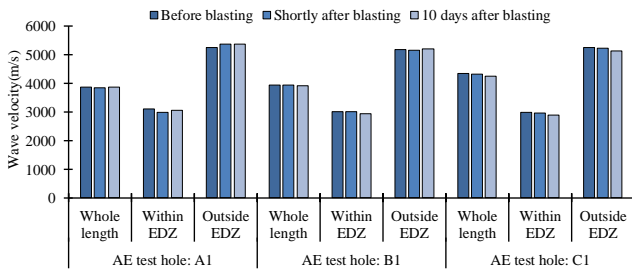


Fig. 10 Comparison of average wave velocity at different depths of surrounding rocks

The EDZ characteristics of the experiment tunnels with an overburden depth over 2000 m are further analyzed and the following three aspects are summarized based on the AE test results.

(1) The EDZ extent of the 2000 m-deep cavern is greatly larger than conventional cases. It is observed from Fig. 8 that, all the curves of wave velocity *versus* rock mass depth can be divided into two parts. The first part corresponds to the areas close to excavation surfaces where wave velocity is low. The second part is the areas far from excavation surfaces where wave velocity is high. The location where wave velocity changes rapidly indicates the boundary of EDZ. Based on Fig. 8, the extent of EDZ is 3.6~4.0 m and accounts for 25.7%~28.6% of the excavation span of experiment tunnels. Fig. 9 gives a further statistics of the distribution of EDZ based on all AE test results. The EDZ extent for 87% test holes exceeds 2.0 m, and for 57% test holes exceeds 3.0 m. This indicates that for 2000 m-deep rock caverns, the blasting and excavation unloading have considerable disturbance on surrounding rock masses. Based on the engineering practices of hydropower underground cavern complexes with large-scale excavation dimensions, the measured extent of EDZ for high sidewalls is generally smaller than 3 m; even the spans of powerhouses are always larger than 30 m and the unfavorable geological conditions are sometimes present at local areas. That is, the maximum extent of EDZ for large-scale underground powerhouses only account for about 10% of the excavation span. The extent of EDZ for the experiment tunnels of Phase II project of Jinping Underground Laboratory, by contrast, is a considerably large magnitude. It is believed that the significant relaxation of surrounding rock masses is a joint effect of great overburden depth (exceeding 2000 m), high natural stress (vertical stress up to 60 MPa), and low strength to stress

ratio (smaller than 2).

(2) The excavation unloading is a key factor that determines the EDZ depth. The average magnitudes of wave velocity corresponding to different ranges of rock mass are summarized and illustrated in Table 1 and Fig. 10. Following findings can be noted.

a. The average magnitudes of wave velocity inside the EDZ is considerably smaller than those outside the EDZ.

b. The comparison of wave velocity curves obtained before and after blasting shows that the depths of EDZ for most test holes remain unchanged.

c. Based on the data of most test holes, the magnitudes of wave velocity inside the EDZ decrease slightly due to blasting, while wave velocity outside the EDZ keeps unchanged.

The above findings determines the roles of blasting effect and excavation unloading effect in the mechanical response of surrounding rock masses subjected to excavation. For blasting load, its primary effect is the reduction of wave velocity of rock masses within EDZ and causes a higher degree of degradation, while has little influences on rock masses outside EDZ. As there is no other effects that may contribute to EDZ, it is inferred that, the only possible effect responsible for rock mass degradation and EDZ generation is excavation unloading of previously implemented excavations. Therefore, the excavation unloading is confirmed a key factor that determines the EDZ extent.

(3) The extent of EDZ is basically time-independent. In order to investigate the time-related characteristics of EDZ extent, AE tests are performed at the different times during the excavation process. The results reveal that the extents of EDZ obtained shortly after blasting and 10 days after blasting are basically the same. This shows that the EDZ evolution caused by blasting and excavation unloading is basically time-independent. Therefore it is unlikely that the failure of time-dependent rupture occurs in surrounding rock masses after drilling and blasting operation.

3. Numerical evaluation of EDZ considering both excavation unloading and blasting loads

3.1 Insights from the analyses of field tests and monitoring data

We obtain following insights based on a comprehensive understanding of the analysis of rock mass vibration monitoring and AE test results.

(1) The essential physical process of drilling and blasting method is to break rocks using extremely high stress, which is generated by dynamites in very short duration. An optimized layout of blasting holes and detonation network makes rocks fracture and spall off along preset path and removes the rocks inside the excavation profile to achieve rock excavation purpose. The blasting load induced by explosion excites blasting seismic wave that transmits through surrounding rocks of cavern to the deep rock masses. The surrounding rocks, as wave transmission medium, will vibrate in a very short period of time and cause stress fluctuation. The instantaneous

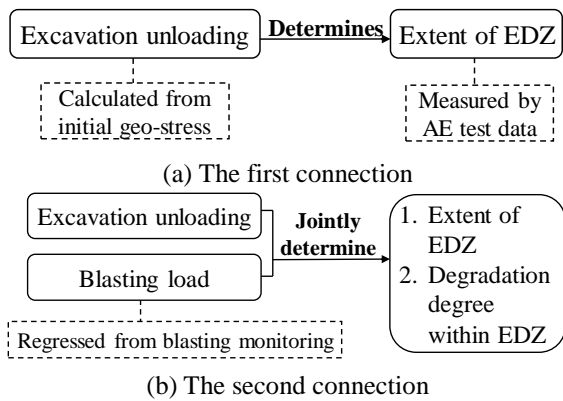


Fig. 11 Connections among excavation unloading, blasting load, extent of EDZ and degradation degree within EDZ

magnitude of blasting load is extremely large and exceeds the strength of rock mass, leading to the failure of rock masses near explosion. However, the action duration on rock masses is very short due to the nature of blasting load. In summary, only part of the rock masses are affected by blasting load in a very short period of time.

(2) The natural stress in rock masses is released and the excavation load is applied to the excavation surface instantly after the removal of rocks within excavation profile. The process is always termed as excavation unloading. Generally, the natural stress magnitude and the excavation scale determine the degree of excavation unloading. The excavation unloading, in comparison with blasting load, is a load that constantly acts on surrounding rocks and requires the surrounding rock masses and their support structures bear the excavation unloading through their own stress redistribution and deformation adjustment.

(3) The drilling and blasting method is the primary approach for rock excavation projects. The surrounding rock masses are subjected to both blasting load and excavation unloading effects and the measured extent of EDZ through AE tests is a comprehensive representation of rock mass mechanical degradation under this joint impact. Although the two loads both contribute to the degradation of rock mass, producing irreversible deformation and reducing bearing capacity, they are remarkably different in terms of action duration and influence mechanism to surrounding rock masses. The blasting load affects rock masses by forcing them vibrate and transmitting blasting seismic wave. The excavation unloading imposes a constant loading effect on the excavation surfaces.

(4) The effects of blasting load and excavation unloading can be divided using proper monitoring and testing methods. Then, the evaluation method for EDZ considering both blasting load and excavation unloading can be proposed. Firstly, rock mass vibration monitoring can quantitatively evaluate the influences of blasting on rock masses and help to regress the blasting input load that corresponds to field vibration magnitude. Then, the natural stress field is regressed based on field stress measurement data, so as to calculate the excavation unloading applied to excavation surfaces. Finally, the extent of EDZ surrounding excavation surfaces is obtained based on AE test results.

(5) As revealed by above analysis on AE test results, the excavation unloading is a key factor that determines the EDZ extent, while the blasting load only increases the degradation degree of rock masses inside the EDZ and does not contribute to the increase of its extent. It is based on this understanding that we can establish the connections among blasting load, excavation unloading, EDZ extent, and degradation degree inside the EDZ. Fig. 11(a) shows the first connection that the excavation unloading determines the extent of EDZ. Fig. 11(b) shows the second connection that the excavation unloading and blasting load jointly determine the extent of EDZ and the degradation degree with EDZ.

3.2 Basic idea and general procedures

Based on the connections described in Fig. 11, we propose a numerical method to evaluate the development and distribution of EDZ for rock caverns considering both blasting load and excavation unloading effects. The numerical method consists of two major steps and they are illustrated in Fig. 12.

Step 1 firstly calculates the excavation unloading based on regression results of initial stress field and excavation plan of the experiment tunnels. This step only considers excavation unloading effect. Then, the damage concept is introduced and the corresponding damage evolution equation is defined. The distribution of damage degree of surrounding rock masses around excavation surfaces is calculated using three-dimensional finite difference method and the extent of EDZ is predicted by an EDZ criterion based on damage concept. Finally, the numerically calculated extent of EDZ is compared with the extent measured by AE tests and the damage constant in the damage evolution equation can be back analyzed to obtain a calibrated damage evolution equation.

Step 2 firstly determines the equivalent blasting load imposed on surrounding rock masses based on regression analysis of blasting monitoring data. Then, the excavation unloading and blasting load are both considered in numerical analysis, which uses the calibrated damage evolution equation. In this way, the degradation characteristics of rock masses subjected to both blasting load and excavation unloading can be included to carry out a detailed description of EDZ development surrounding the cavern excavation. Finally, the stability assessment of rock caverns can be conducted based on the EDZ distribution.

3.3 Step 1: Determine damage evolution equation for describing rock mass degradation

3.3.1 Description of rock mass degradation using damage concept

Under the influences of external load or environmental factors, the internal mesoscopic cracks initiate, propagate, and form macroscopic cracks, leading to irreversible changes and causing the degradation of both mechanical properties of materials and bearing capacities of structures. The mechanism regarding crack development and material or structural degradation under external impacts is generally termed as damage. When excavating rock caverns, the

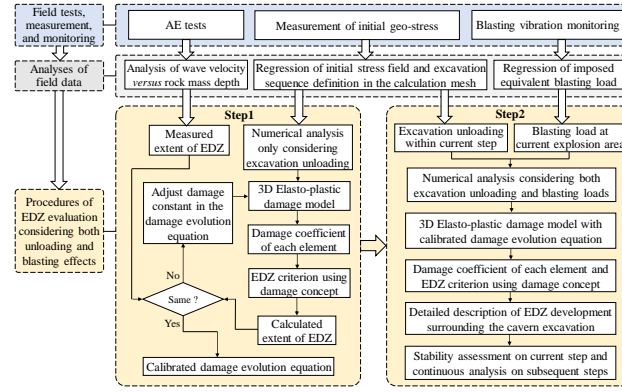


Fig. 12 A flowchart describing the basic idea and major procedures of the EDZ evaluation method considering both unloading and blasting effects: within Step 1, the calibrated damage evolution equation is obtained based on the measured extent of EDZ; within Step 2, numerical analysis is conducted considering both unloading and blasting loads using the calibrated damage evolution equation

blasting load and excavation unloading leads to stress redistribution of surrounding rock masses. Some internal fissures and cracks of a mesoscopic scale take on irreversible changes such as open and expand driven by external load. The mesoscopic transformation of internal structures of rock masses reduces their macroscopic bearing capacity and integrity.

As the definition of damage is highly consistent with the mesoscopic transformation of internal structures of rock masses during their stress redistribution process, many scholars employ the damage concept to conduct both qualitative and quantitative analysis of rock mass relaxation induced by excavation unloading. This paper also uses the damage concept to study the EDZ.

3.3.2 Selection of damage evolution equation for rock mass degradation

There are several commonly adopted damage evolution equations for rock and rock-like materials. When Frantziskonis and Desai (1987) studied the crack issue of rock and concrete, they considered that the cracks initiate under external load and the stress in the cracking area will be partly released, causing the reduction of stress level and leading to stress damage zone. They believed that elastic deformation of materials does not generate damage and no failure takes place under hydrostatic pressure. The main reason for material damage depends on the partial tensor of plastic strain. When rock masses are degraded, their stress level and physical properties decrease as the plastic strain increases. The damage degree of materials is also higher with the increase of plastic strain.

The propagation and development of internal cracks will be very fast when a material is about to reach its strengths. The variation rate of damage degree, under this circumstance, can be described using an exponential function. In three-dimensional conditions, the damage evolution equation is given as

$$D = 1 - \exp(-Re_D) \quad (1)$$

where D is damage coefficient, $e_D = \sqrt{\varepsilon_{ij}^p \cdot \varepsilon_{ij}^p}$, and R is the damage constant of material.

3.3.3 EDZ determination using damage concept

The wave velocity variation along the depth of rock masses can help to determine the extent of EDZ because this index is an effective indicator of degradation degree of surrounding rock masses. Here, the wave velocity obtained by AE test and the damage coefficient are combined to propose a criterion that determine the extent of EDZ (Zhang *et al.* 2017).

The longitudinal wave velocity is calculated using

$$C_p = \sqrt{\frac{E(1-\mu)}{\rho(1+\mu)(1-2\mu)}} \quad C_{p1} = \sqrt{\frac{E_1(1-\mu)}{\rho_1(1+\mu)(1-2\mu)}} \quad (2)$$

where C_p and C_{p1} refer to wave velocity for undisturbed rock masses and degraded rock masses, respectively. Divide C_p by C_{p1} , we have

$$\frac{C_{p1}}{C_p} = \sqrt{\frac{\rho E_1}{\rho_1 E}} \quad (3)$$

Based on the definition of damage, the damage coefficient D is a reduction factor of the deformation modulus of the undisturbed rock masses. Therefore we have

$$E_1 = (1 - D)E \quad (4)$$

where E_1 and E are the deformation modulus for undisturbed rock masses and degraded rock masses, respectively. Based on Eqs. (3)-(4), we have

$$D = 1 - \frac{E_1}{E} = 1 - \frac{\rho_1}{\rho} \left(\frac{C_{p1}}{C_p} \right)^2 \quad (5)$$

where ρ_1 and ρ are densities for undisturbed rock masses and degraded rock masses, respectively. The volumetric strain θ is defines as

$$\theta = \frac{V_1 - V}{V} = \frac{\rho}{\rho_1} - 1 \quad (6)$$

where V_1 and V are volumes. It also can be calculated by

$$\theta = \varepsilon_1 + \varepsilon_2 + \varepsilon_3 \quad (7)$$

where ε_1 , ε_2 , and ε_3 are the three principal strains. Put (6) into Eq. (5), we have

$$D = 1 - \frac{1}{1 + \theta} \left(\frac{C_{p1}}{C_p} \right)^2 \quad (8)$$

According to the engineering practices in China, the rock masses, in which wave velocity decreases 10% and above compared to the velocity measured in undisturbed rock masses, can be judged as relaxation zone. That is to say, if the ratio of the wave velocity C_{p1} of concerned rock mass to the wave velocity C_p of undisturbed rock masses is lower than 0.9 ($C_{p1} / C_p < 0.9$), then the concerned rock mass is determined as EDZ. Therefore, we put this quantitative criterion into Eq. (8) and obtain a damage coefficient related EDZ criterion as

$$D \geq 1 - (0.9)^2(1 + \theta)^{-1} = 1 - 0.81(1 + \theta)^{-1} \quad (9)$$

If Eq. (8) does not consider volumetric variation, then $\theta = 0$ and Eq. (9) is further written as

$$D \geq 0.19 \quad (10)$$

Based on Eqs. (9)-(10), the threshold value of damage coefficient that determines the boundary of EDZ can be obtained. Thus, the EDZ criterion is established.

As is shown in Fig. 8, the average wave velocity inside the EDZ is considerably smaller than that outside the EDZ. The wave velocity increases rapidly to a fairly high level when the measurement extent exceeds the EDZ range. This shows that although the relaxation extent of the experiment tunnels in the Phase II project of Jinping Underground Laboratory is larger and the degradation degree of rock masses inside the EDZ is considerable, the wave velocity is able to restore the undisturbed magnitude for rock masses outside the EDZ. Based on the derivation process of Eq. (8), we know that once the wave velocity magnitude exceeds 90% of the magnitude measured in undisturbed rock masses, the rock masses can be considered undisturbed. Therefore, Eqs. (9)-(10) are able to determine the extent of EDZ for the studied rock cavern.

3.3.4 Back analysis of damage constant in damage evolution equation

The distribution of damage coefficient of the surrounding rock masses can be calculated based on three-dimensional finite difference method considering damage evolution equation. By combining Eqs. (9) and (10), the range of EDZ and its extent can be determined. Then, the calculated extent of EDZ and its measured extent is compared. By adjusting the index of damage constant and performing repeated numerical analysis, the calculated extent of EDZ will gradually approach the measured value. Finally, the damage constant can be back analyzed and the calibrated damage evolution equation is obtained.

3.4 Step 2: Numerical analysis of EDZ and stability assessment considering both blasting load and excavation unloading

3.4.1 Regression of blasting load based on rock mass vibration monitoring data

The rocks around blasting holes are crushed, thrown, and accumulated under the shock wave produced by

blasting. The surrounding rock masses, based on their response characteristics, can be classified into flow plastic zone, elasto-plastic zone, and elastic zone. As the explosion only has significant impacts to rocks within a limited range, a boundary around the blasting holes can be assumed. Rocks are crushed and fractured inside the range of the boundary and remain continuously deformation characteristics outside the range. Therefore, according to the Saint-Venant principle, the influence of blasting on rock masses outside the boundary can be equivalent to a load that is applied to the surfaces of the boundary. Therefore, the calculation results of stress distribution and vibration for rock masses outside the boundary should be equivalent to the results of detonation blasting calculation in which blasting holes and dynamite explosion process are finely simulated. According to Lu's study (Lu *et al.* 2011), such a boundary is termed as equivalent elastic boundary and its range can adopt the crushing and fractured extent around a blasting hole. Generally, the radius of crushing area is 3~5 times of the radius of column charge and the radius of fractured area is 10~15 times of the radius of column charge.

Based on above conclusion, the blasting effect is considered as a load applied to the excavation surfaces of cavern. The blasting load is regressed based on rock mass vibration monitoring data. The basic procedures of this regression process is described as below.

- (1) Establish calculation mesh and perform excavation calculation that only considers excavation unloading.
- (2) Select a characteristic curve of load *versus* duration as the input time history of blasting load and apply the load to the excavation surfaces of current blasting step.
- (3) Perform time history analysis and monitor the vibration response of characteristic location in the calculation mesh.
- (4) Summary the PPV of each monitoring location and compare the calculated PPV distribution with the measure data.
- (5) Adjust the peak value of input blasting load and repeat time history analysis. The regression of blasting load is considered completed when the calculated PPV distribution is basically consistent with the measured data.

3.4.2 Numerical simulation of excavation and blasting process based on calibrated damage evolution equation and regressed blasting load

As the damage evolution equation is calibrated based on AE test results and the blasting load is also regressed based on rock mass vibration monitoring data, the primary factors that affect the stability of surrounding rock masses have been quantitatively determined. After that, numerical simulation can be carried out according to the actual piecewise construction process of underground caverns to reflect the actual mechanical response of surrounding rock masses under excavation unloading and blasting load effect.

3.4.3 Rock mass stability based on the calculation results of EDZ

The damage coefficient for each element can be calculated during the simulation of excavation and blasting process of underground caverns. Then, the extent of EDZ

can be determined according to Eqs. (9) and (10). The obtained EDZ result, including its extent and damage coefficient distribution, indicates the overall stability of rock masses surrounding the underground caverns and provides much more information than the AE test results do. Therefore, a comprehensive evaluation can be conducted towards the rock mass stability condition under both excavation unloading and blasting load effect, combining other obtained calculation indexes such as rock mass deformation and rock mass stress.

4. Application of the evaluation method to the 2000 m-deep rock cavern

4.1 Initial calculation conditions

4.1.1 Calculation mesh

The #3 experiment tunnel at the Phase II of Jinping Underground Laboratory is selected and the calculation mesh is discretized as shown in Figs. 13 and 14. The covering range of the model is $X \times Y \times Z = 120 \text{ m} \times 90 \text{ m} \times 120 \text{ m}$. The X axis is perpendicular to the longitudinal direction of tunnel, the Y axis is parallel to the longitudinal direction, and the Z axis is the vertical direction. Eight-node hexahedral element is used and totally 486 618 nodes and 473 616 elements are discretized. In order to meet the requirement of subsequent blasting calculation, finer elements with smaller dimensions are used around the tunnel. The maximum element edge length surrounding the cavern is restricted in accordance with the requirement of a dynamic calculation. The boundary condition of the mesh uses the quiet boundary condition, which absorbs the wave transmitted from the inner mesh. FLAC^{3D} software is used here to conduct the calculation.

4.1.2 Initial geo-stress and rock mass properties

Based on the results of initial geo-stress measurements, three stress components, which are σ_x , σ_y , and σ_z , are applied to the model. The stress magnitudes along X, Y, and Z direction of the model is 39.7 MPa, 34.9 MPa and 58.3 MPa, respectively. The adopted rock mass parameters are given in Table 2. It should be noted that the parameters in Table 2 are only initial values that are used in the model. When the proposed elasto-plastic damage model is considered, the rock mass parameters will be updated.

4.1.3 Input blasting load

The characteristic curve of load *versus* duration selects the triangle curve form plotted in Fig. 15, in which the ascending duration is 1.0 ms and the descending duration is 7.0 ms. Based on the method introduced in 3.4.1, the blasting load is regressed by adjusting the peak load of the triangle curve P_{b0} , which is plotted in Fig. 15.

4.1.4 Calculation schemes

To present a comprehensive implementation effect of the proposed method, four calculation schemes are designed and listed in Table 3. Following sections present the results of different calculation schemes and their comparisons.

4.2 Determination of damage evolution equation: Scheme A result

The damage constant is firstly selected based on

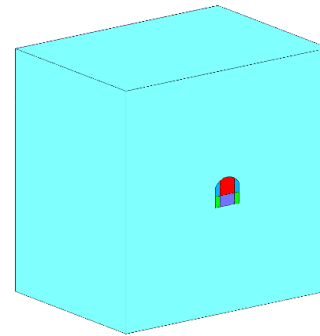


Fig. 13 Calculation model containing excavation steps

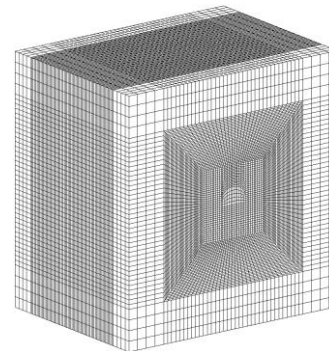


Fig. 14 Calculation mesh

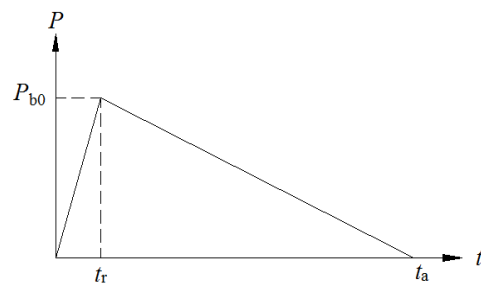


Fig. 15 Selected time history form for blasting load

Table 2 Mechanical parameters of rock masses

Density / $\text{kg} \cdot \text{m}^{-3}$	Deformation modulus / GPa	Poisson's ratio	Cohesion / MPa	Internal friction angle / $^\circ$
2700	56.2	0.24	3	38

Table 3 Summary of calculation schemes

Scheme	Calculation content	Constitutive model	Calculation purpose
A	Sequential excavation	Elasto-plastic damage model	Calibration of damage constant to determine damage evolution equation
B	Sequential excavation	Ideal elasto-plastic model	Comparison with Scheme A to prove the effectiveness of the damage model
C	Blasting vibration	Elasto-plastic damage model with calibrated damage constant	Regression of input blasting load based on monitoring data
D	Sequential excavation and blasting	Elasto-plastic damage model with calibrated damage constant	Stability evaluation considering both blasting and excavation effects

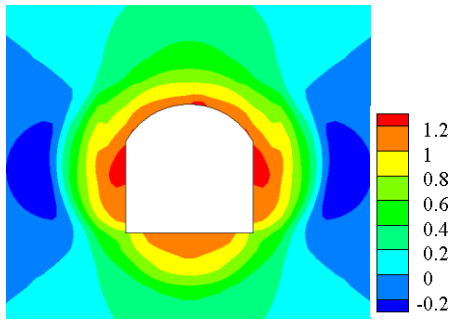


Fig. 16 Contours of volumetric strain distribution(unit: 10^{-3})

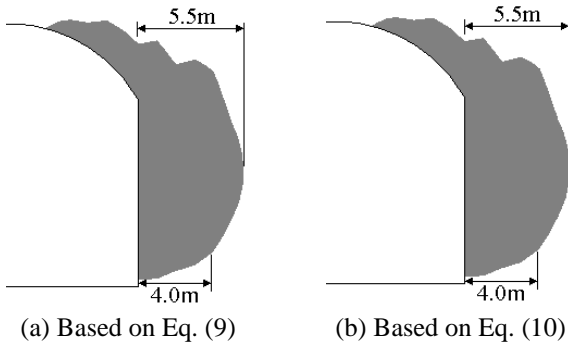


Fig. 17 Different EDZ determination results using calibrated damage evolution equation

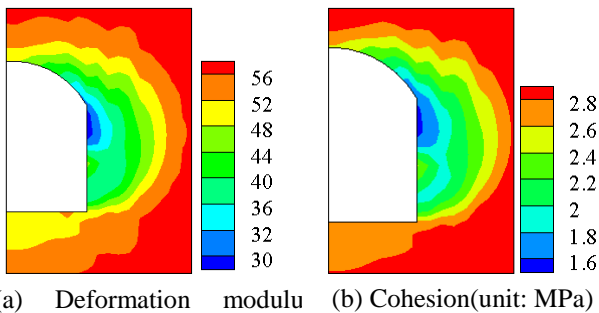


Fig. 18 Distribution of rock mass mechanical parameters updated by elasto-plastic damage model

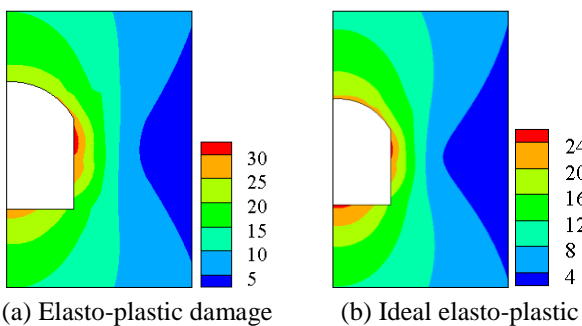


Fig. 19 Deformations using different constitutive models (unit: mm)

previous related calculation experiences. Adjustments are then made based on the calculated extent of EDZ and field measurement results. By repeated calculation and adjustment, the difference of calculated and measured EDZ extents becomes smaller and smaller so the damage

constant is calibrated and the damage evolution equation is determined. It should be noted that, based on Table 1, the measured maximum EDZ extent of 4.0 m was obtained at the testing holes that are 1 m above the cavern floor. Therefore, the calculation result adopts the same location with the field measurement as the reference of calibration. The calculation results plot two values of EDZ extent, they are the reference location and the maximum extent location. The results are analyzed as below.

Fig. 16 plots the contours of volumetric strain corresponding to the completion of cavern excavation, where positive values refer to volume increase and negative values refer to volume decrease. The maximum strain indicating the volume increase is 0.0013 and the minimum strain indicating the volume decrease is -0.00035.

As the calculation results of the cavern are axisymmetric with respect to the centerline of the cavern, only the results of the right left part are displayed hereinafter. Fig. 17 plots the EDZ determination results using the same calibrated damage evolution equation but with different EDZ determination equations. It is compared that the distributions of EDZ are almost identical to each other and the extents of EDZ at both reference location and maximum extent location are the same as well, indicating the volumetric variation of rock masses subjected to excavation is tiny and can be neglected.

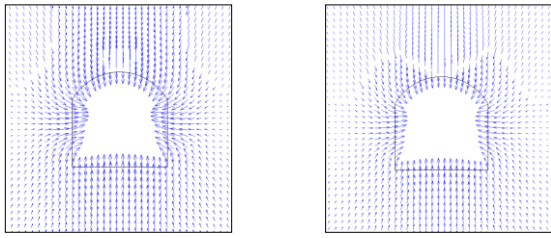
In general, the calculation results not only match the field measured extent of EDZ, but also provide a quantitative description of rock mass degradation subjected to excavation effect, while traditional ideal elasto-plastic models fails to do so. Therefore, it is considered rational to adopt the proposed elasto-plastic damage model with a calibration operation on the damage constant.

Fig. 18 plots the mechanical parameter distribution. The contours show that the closer the rock masses are to the excavation surfaces, the more obvious the degradation will be. The minimum deformation modulus and cohesion values reach 28.8 GPa and 1.54 MPa respectively, accounting for 51.2% and 51.3% of their original values. The rock mass degradation is more significant at sidewalls than crown and floor.

4.3 Comparison of results using different constitutive models: Scheme A and B results

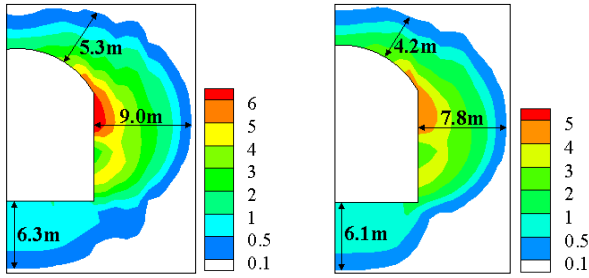
The following compares the results achieved by different constitutive model. Fig. 19 shows that the maximum deformations are 33.37 mm and 25.78 mm, respectively using the elasto-plastic damage model and the ideal elasto-plastic model. Fig. 20 reveals a similar deformation vector distribution characteristic between the two results. Fig. 21 measures the extents of plastic zone surrounding the cavern. For the elasto-plastic damage model result, the plastic zone extents are 5.3 m, 9.0 m, and 6.3 m at the crown, sidewall, and floor, respectively. For the ideal elasto-plastic model, the plastic zone extents are 4.2 m, 7.8 m, and 6.1 m, respectively. By comparing the data, the results of plastic zone extent predicted by the elasto-plastic damage model are 1.1 m~1.2 m or 3.3%~26.2% larger than the results of ideal elasto-plastic model.

In general, the calculation results achieved by the



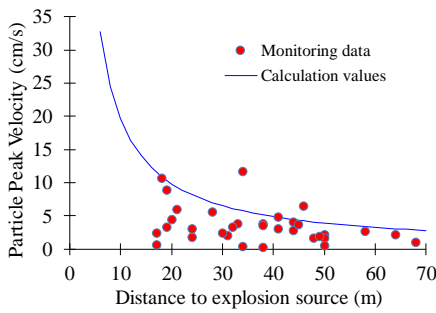
(a) Elasto-plastic damage (b) Ideal elasto-plastic

Fig. 20 Deformation vectors using different constitutive models: Displayed in a same scaling ratio

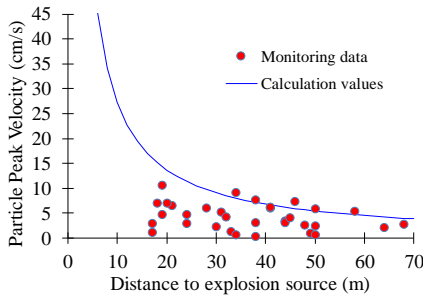


(a) Elasto-plastic damage (b) Ideal elasto-plastic

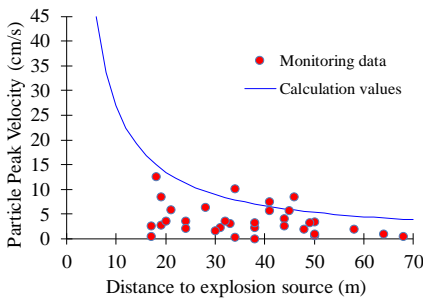
Fig. 21 Plastic zones using different constitutive models: displayed by equivalent plastic strain (unit: 10^{-3})



(a) x direction



(b) y direction



(c) z direction

Fig. 22 Comparisons of monitored and calculated PPV along different directions

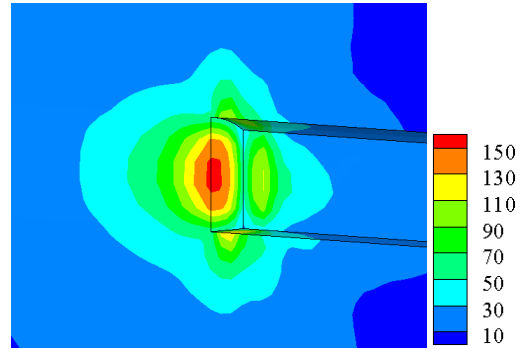


Fig. 23 PPV distribution of the right half of the calculation mesh: corresponding to 1st excavation step (unit: cm/s)

constitutive model considering rock mass degradation effect show larger deformations and plastic zone extents than the results achieved by traditional ideal elasto-plastic constitutive model. In particular, the crown and sidewall of cavern are observed more sensitive to the choice of constitutive model, where a larger increase of deformations and plastic zone extents are identified.

4.4 Blasting load regression and blasting vibration results: Scheme C results

The input blasting load is regressed using fielding blasting monitoring data. As the excavation and blasting construction was conducted progressively, the input blasting load is regressed within each excavation step. Fig. 22 shows that the regressed PPV distributions with respect to 1st excavation step along different axial directions are consistent with the monitored data. Fig. 23 shows the corresponding regressed PPV contours of the right half of the calculation mesh. The calculated maximum PPV values on the excavation surfaces in x, y, z directions are 109.4 cm/s, 155.1 cm/s, and 125.6 cm/s, respectively.

For the remaining 2nd, 3rd, and 4th excavation steps, the input blasting load is likewise regressed using the blasting vibration data collected at corresponding step. Therefore the input blasting load reflecting the field vibration level is obtained and then can be used as an initial load condition in the subsequent calculation Scheme D, which includes both excavation unloading and blasting effect.

4.5 Sequential excavation and blasting: Scheme D results

Based on the regression results of Scheme C, the obtained blasting loads are considered by restarting a numerical calculation using the elasto-plastic damage model with the calibrated damage constant. The results of each excavation step are summarized.

Fig. 24 plots the damage coefficient curve *versus* the depth of surrounding rock masses at the completion of 1st excavation step. It is observed that the inclusion of blasting effect produces larger rock mass damage and the difference of damage coefficient is greater when it is closer to the excavation surfaces. Such result is consistent with the conclusion drawn from the analysis of AE results, which

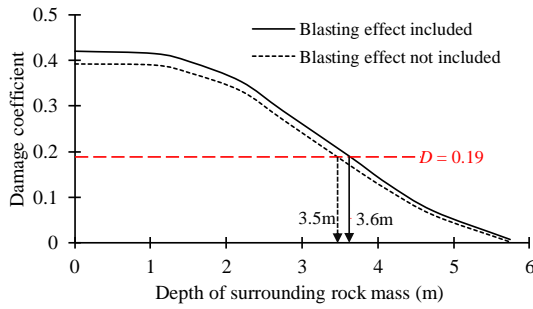


Fig. 24 Damage coefficient curves versus depth of surrounding rock masses: 1st excavation step

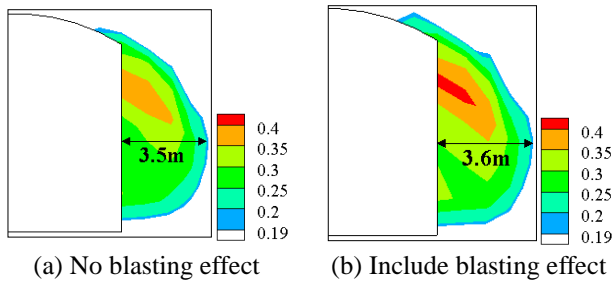


Fig. 25 Distributions of damage coefficient that satisfy $D \geq 0.19$: 1st excavation step

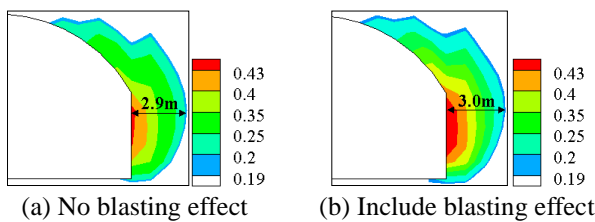


Fig. 26 Distributions of damage coefficient that satisfy $D \geq 0.19$: 2nd excavation step

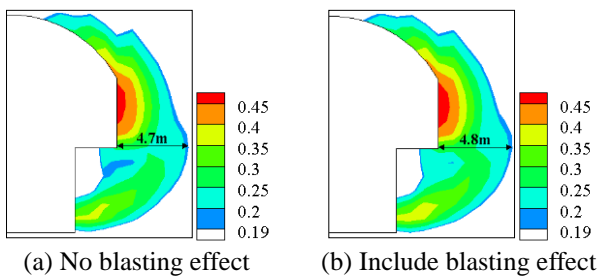


Fig. 27 Distributions of damage coefficient that satisfy $D \geq 0.19$: 3rd excavation step

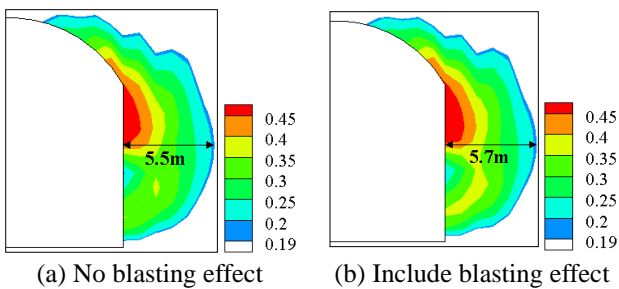


Fig. 28 Distributions of damage coefficient that satisfy $D \geq 0.19$: 4th excavation step

discover that the blasting load will cause a higher degree of degradation within the EDZ range.

Meanwhile, the EDZ extents, determined by the $D \geq 0.19$ criterion and plotted by Fig. 25, are 3.6 m and 3.5 m, respectively, indicating a very slight increase due to the inclusion of blasting effect. The results of the remaining excavation steps also support this finding. The inclusion of blasting load produces 0.1 m, 0.1 m, and 0.2 m increments of EDZ extent for 2nd, 3rd, and 4th steps, respectively, as shown in Figs. 26-28.

4.6 Stability evaluation of rock masses

The rock mass stability, based on the calculation results considering both excavation unloading and blasting effect, can be evaluated in terms of following aspects.

- (a) The deformations of surrounding rock masses are not large, so the deformation related failure will not occur.
- (b) The AE test results show that the rock mass relaxation does not exhibit time dependent effect, so it is stable after excavation.
- (c) The blasting vibration monitoring results show that the rock mass vibration is at a normal level and agrees with the general laws of rock mass response.

(d) The maximum extent of EDZ revealed by calculation is 5.7m. Although it is larger than the extent revealed by AE test, it is smaller than the designed 6m long anchor bolts.

In summary, the overall stability of the studied cavern at the Phase II of Jinping Underground Laboratory is evaluated in a basically favorable condition.

5. Discussions

By studying the field measurement data and numerical simulation results, it is necessary to discuss the following aspects so as to provide a more comprehensive insight regarding the blasting effect, the proposed method, and some other factors that should be emphasized.

5.1 The role of blasting effect

As indicated by the analysis of AE test results, the blasting effect mainly produces a higher degree of rock mass degradation within the EDZ range, while has little contribution to the extension of EDZ. The numerical simulation result, on one hand, validates the impact of blasting load on rock masses within the EDZ range, but on other hand, indicates that the inclusion of blasting load will lead to a slight extension of EDZ.

The above seemingly contradictory conclusions, by a further detailed comparison, are actually caused by the measurement accuracy of field AE test. As is described in the scheme of AE test, the data of wave velocity is collected every 0.2 m, thus resulting in a measurement accuracy of 0.2 m. Such error is exactly the maximum difference caused by inclusion or exclusion of blasting load revealed by numerical simulation.

Therefore, the role of blasting effect should be improved

based on a more rational understanding, combining the field test results and numerical simulation results. That is, the blasting load not only produces a higher degree of rock mass degradation within the EDZ range, but also leads to a slight increase of EDZ extent. However, comparing the major influences caused by excavation unloading, the impact caused by blasting is minor.

5.2 The applicability of proposed numerical method

The proposed numerical method for evaluation of EDZ considers both excavation unloading and blasting effect and especially features a calibration operation of damage constant and a regression process of blasting load. The method and related implementing procedures are proposed based on the characteristics of field measurement results.

For other rock excavation projects with similar field measurement characteristics, the proposed method is also applicable. These characteristics include the independence of rock mass responses with respect to time and minor impact caused by blasting load compared to excavation unloading. On the other hand, if field revealed data exhibit different characteristics, such as time dependent effect and significant blasting-related impact, then the proposed numerical method should be modified accordingly to reflect the variation.

5.3 The potential effect of geological discontinuities

The #3 experiment tunnel of Jinping Underground Laboratory is primarily focused in this paper. The collected field measurement results, especially the AE test data, reflect local geological conditions and rock mass structure characteristics corresponding to this specific cavern. As there is no controlling geological defects for the studied #3 experiment tunnel, their adverse effects on rock mass stability under excavation and blasting were not included through neither qualitative analysis of field measurement data nor quantitative evaluation of numerical simulation results.

Based on our experiences, the influences of blasting load on rock mass stability may vary depending on the features of rock mass structure so the potential effect of geological discontinuities remains a live issue and calls for further studies.

6. Conclusions

The issue of field measurement of EDZ and its numerical simulation method considering both excavation unloading and blasting load effects are carefully studied based on a 2000 m-deep rock cavern. Following conclusions can be drawn.

- The extent of EDZ of the rock cavern, based on the AE test results, is revealed 3.6 m~4.0 m, accounting for 28.6% of the cavern span. The EDZ extent is considerably larger than rock caverns of conventional overburden depth and the significant relaxation can be viewed as a joint effect of great overburden depth, high natural stress, and low strength to stress ratio.

- The proposed numerical simulation method for EDZ determination features a calibration operation of damage constant, which contributes to an elasto-plastic damage constitutive model, and a regression process of blasting load using field blasting vibration monitoring data. So it combines the excavation unloading and blasting load effects and provides reasonable results consistent with field measurement findings. It is concluded that the blasting load not only produces a higher degree of rock mass degradation within the EDZ range, but also leads to a slight increase of EDZ extent. But its impact to rock mass stability is minor, compared to the major influences caused by excavation unloading.

- The reported case of the 2000 m-deep rock cavern and its corresponding analyses are hoped to broaden the understanding of mechanical behaviors of rock masses subjected to excavation and blasting at great depth. The presented numerical simulation method for EDZ determination considers both excavation unloading and blasting load effects. As demonstrated by the studied case, it can be an available and feasible evaluation method for rock caverns with similar characteristics.

Acknowledgements

Financial supports from the National Key Research and Development Program of China (No. 2016YFC0402008), the National Natural Science Foundation of China (Nos. 51539002, 51779018, 51609018), and the Basic Research Fund for Central Research Institutes of Public Causes (Nos. CKSF2017054/YT, CKSF2017014/YT, CKSF2016272/YT) are greatly acknowledged.

References

- Almusallam, T.H., Elsanadedy, H.M., Abbas, H., Alsayed, S.H. and Al-Salloum, Y.A. (2010), "Progressive collapse analysis of a RC building subjected to blast loads", *Struct. Eng. Mech.*, **36**(3), 301-319.
- Bayraktar, A., Türker, T., Altunışık, A.C. and Sevim, B. (2010), "Evaluation of blast effects on reinforced concrete buildings considering operational modal analysis results", *Soil Dyn. Earthq. Eng.*, **30**(5), 310-319.
- Bobet, A. (2009), "Application to excavation damage zone and rockbolt support", *Rock Mech. Rock Eng.*, **42**(2), 147-174.
- Chen, J., Jiang, D., Jiang, D.Y., Fan, J.Y. and He, Y. (2016), "The mechanical properties of rock salt under cyclic loading-unloading experiments", *Geomech. Eng.*, **10**(3), 324-334.
- Christaras, B. and Chatziangelou, M. (2014), "Blastability quality system (BQS) for using it, in bedrock excavation", *Struct. Eng. Mech.*, **51**(5), 823-845.
- Frantziskonis, G. and Desai, C.S. (1987), "Constitutive model with strain softening", *Int. J. Solid. Struct.*, **23**(6), 733-750.
- Gholizadeh, S., Leman, Z. and Baharudin, B.T.H.T. (2015), "A review of the application of acoustic emission technique in engineering", *Struct. Eng. Mech.*, **54**(6), 1075-1095.
- Han, Y.Z. and Liu, H.B. (2016), "Failure of circular tunnel in saturated soil subjected to internal blast loading", *Geomech. Eng.*, **11**(3), 421-438.
- Jeon, S., Kim, T.H. and You, K.H. (2015), "Characteristics of crater formation due to explosives blasting in rock mass",

- Geomech. Eng.*, **9**(3), 329-344.
- Jin, P., Wang, E. and Song, D. (2017), "Study on correlation of acoustic emission and plastic strain based on coal-rock damage theory", *Geomech. Eng.*, **12**(4), 627-637.
- Lesparre, N., Gibert, D., Nicollin, F., Nussbaum, C. and Adler, A. (2013), "Monitoring the excavation damaged zone by three-dimensional reconstruction of electrical resistivity", *Geophys. J. Int.*, **195**(2), 972-984.
- Li, H.B., Liu, M.C., Xing, W.B., Shao, S. and Zhou, J.W. (2017), "Failure mechanisms and evolution assessment of the excavation damaged zones in a large-scale and deeply buried underground powerhouse", *Rock Mech. Rock Eng.*, **50**(7), 1883-1900.
- Li, S.J., Feng, X.T., Li, Z.H., Chen, B.R., Jiang, Q., Wu, S.Y., Hu, B. and Xu, J.S. (2011), "In situ experiments on width and evolution characteristics of excavation damaged zone in deeply buried tunnels", *Sci. China Technol. Sci.*, **54**(s1), 167-174.
- Liang, M., Lu, F., Zhang, G. and Li, X. (2017), "Design of stepwise foam claddings subjected to air-blast based on voronoi model", *Steel Compos. Struct.*, **23**(1), 107-114.
- Liu, H.B., Xiao, M. and Chen, J.T. (2013), "Parametric modeling on spatial effect of excavation-damaged zone of underground cavern", *J. Central South Univ.*, **20**(4), 1085-1093.
- Lu, W.B., Yang, J.H. and Chen, M. (2011), "Mechanism and equivalent numerical simulation of transient release of excavation load for deep tunnel", *Chin. J. Rock Mech. Eng.*, **30**(6), 1089-1096.
- Oncu, M.E., Yon, B., Akkoyun, O. and Taskiran, T. (2015), "Investigation of blast-induced ground vibration effects on rural buildings", *Struct. Eng. Mech.*, **54**(3), 545-560.
- Song, Z.P., Li, S.H., Wang, J.B., Sun, Z.Y., Liu, J. and Chang, Y.Z. (2018), "Determination of equivalent blasting load considering millisecond delay effect", *Geomech. Eng.*, **11**(5), 745-754.
- Tokiwa, T., Tsusaka, K., Matsubara, M., Ishikawa, T. and Ogawa, D. (2013), "Formation mechanism of extension fractures induced by excavation of a gallery in soft sedimentary rock, Horonobe area, Northern Japan.", *Geosci. Front.*, **4**(1), 105-111.
- Toy, A.T. and Sevim, B. (2017), "Numerically and empirically determination of blasting response of a RC retaining wall under TNT explosive", *Adv. Concrete Construct.*, **5**(5), 493-512.
- Wang, H.P., Li, Y., Li, S.C., Zhang, Q.S. and Liu, J. (2016), "An elasto-plastic damage constitutive model for jointed rock mass with an application", *Geomech. Eng.*, **11**(1), 77-94.
- Xue, X., Yang, X. and Zhang, W. (2013), "Damage analysis of arch dam under blast loading", *Comput. Concrete*, **12**(1), 65-77.
- Yang, J.H., Lu, W.B., Hu, Y.G., Chen, M. and Yan, P. (2015), "Numerical simulation of rock mass damage evolution during deep-buried tunnel excavation by drill and blast", *Rock Mech. Rock Eng.*, **48**(5), 2045-2059.
- Zhang, Y.T., Ding, X.L., Huang, S.L., Pei, Q.T. and Wu, Y.J. (2017), "A framework for modelling mechanical behavior of surrounding rocks of underground openings under seismic load", *Earthq. Struct.*, **13**(6), 519-529.